Flux Creep Investigation in $Bi_2Sr_2CaCu_2O_{8+\delta}$ High-Temperature Superconductor

G. R. Blanca*, J. Ronulo, G. Dumlao, and R. Sarmago
Condensed Matter PhysicsLaboratory,
National Institute of Physics, University of the Philippines,
Diliman, Quezon City, 1101
E-mail: gsblanca@up.edu.ph

ABSTRACT

The flux creep process in a *c*-axis $Bi_2Sr_2CaCu_2O_{8+\delta}$ thin film was investigated at different temperatures and applied fields using the Kim-Anderson (KA) approach. The peaked behavior shown in the magnetoresistance profile was attributed to the competing mechanisms of flux motion and sample-intrinsic transition near T_c.Within the temperature range where the competition occurs, U increases with temperature and consequently a decrease in the superconducting volume corresponds to a decrease in the flux creep. Moreover, the flux creep potential barrier varies with applied current I at all temperatures consistent with the KA model.

INTRODUCTION

Investigations of the flux-creep process in type-II superconductors reveal important information about the interaction of vortices with pinning centers and among the vortices themselves (Landau & Ott, 2001). Studies of this type are essential in controlling the properties in the mixed state as well as in the realization of high-current applications. The magnetic flux motion in high-temperature superconductors (HTSCs) is extremely complex and this presents a problem in the understanding of dissipation mechanism in these materials (Poole et al., 1995). However, after reconsideration of the available data, Landau and Ott (2001) recently showed that low-temperature flux creep and vortex motion close to the superconducting critical temperature (T_C) may very well be explained using the Kim-Anderson description if a realistic profile of the pinning potential was taken into account. Furthermore, they showed that the specific features of vortex dynamics, such as the irreversibility line and a vortex-glass transition, not only may be explained by employing the Kim-Anderson model, but are a direct consequence of the simple model.

This paper investigates the flux creep process in $Bi_2Sr_2CaCu_2O_{8+d}$. An analysis of the magnetoresistance was initially made to determine the exclusive flux regime. The current dependence of the potential barrier was obtained and analyzed using the Kim-Anderson model. Direct transport measurements were performed on the sample to obtain resistance and *I-V* profiles.

METHODOLOGY

Resistance measurements at varying fields were done on a *c*-axis $Bi_2Sr_2CaCu_2O_{8+d}$ thin film grown via combined liquid-assisted powder deposition and liquid-phase sintering process (Ambanta, 2004). Standard four-point probe method was utilized in the transport measurements with pressed indium solder on gold wires

*Corresponding author

 Science Diliman (July-December 2004) **16:2**, 26–30

as contacts. Isothermal current-voltage (I-V) measurements were also obtained at different temperatures with magnetic field applications of 0.1 and 1.25 T and a transport current of 10 mA.

Magnetoresistance profiles are presented in this work using

$$\text{Magnetoresistance}\ (\Omega) = R(B, I) - R(B = 0, I), \quad (1)$$

where $R(B)$ corresponds to resistance measurements with an applied magnetic field of certain magnitude B and transport current I, and $R(B=0)$ pertains to zero-field resistance measurements with transport current I.

RESULTS AND DISCUSSION

The resistance-temperature profiles of the sample shown in Fig. 1 reveals the sample's superconducting critical temperature T_c indicated at 87 K. Upon the application of increasing magnetic field, a very pronounced broadening of the transition region was observed. This is expected due to the increasing number of mobile flux lines, corresponding to a higher applied magnetic field.

The magnetoresistance profiles were obtained to determine the flux creep regime. The magnetoresistance exhibits a peaked behavior which depicts the nature of dissipation in the mixed state of the high temperature superconducting sample. We define four distinct region of the magnetoresistance profile as illustrated in Fig.

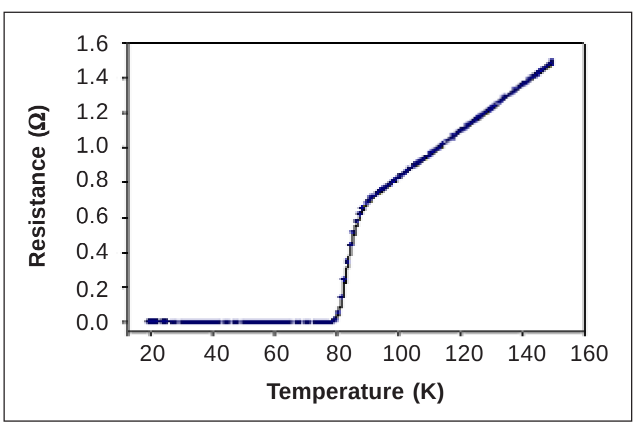

Fig. 1. The broadening of the transition region with increasing applied magnetic field perpendicular to the transport current.

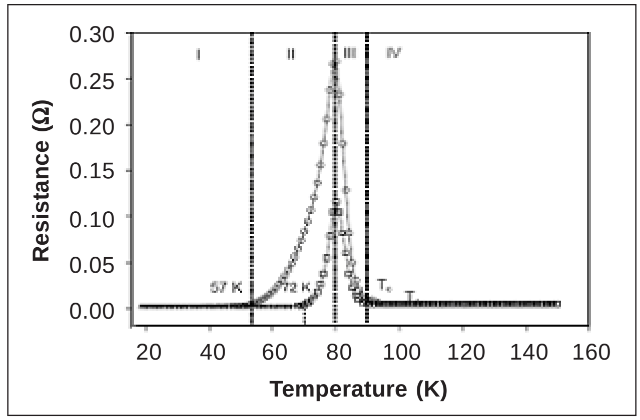

Fig. 2. The increasing magnetoresistance with temperature in Region II corresponds to the flux creep regime.

2. Region I corresponds to the regime of zero dissipation, which may include the Meissner state at low temperature, and the vortex glass state, the regime of immobile flux lines due to insurmountable potential barrier, at higher temperature. Region II, the region of increasing magnetoresistance with temperature, should correspond to the flux creep regime, where vortices hop out of pinning sites via thermal activation, causing dissipation that increases with temperature. The temperature-coinciding maxima of the magnetoresistance profiles, the boundary between regions II and III, occur at 80 K, the exact same temperature when the $Bi_2Sr_2CaCu_2O_{8+d}$ sample begins its intrinsic transition to the normal state. This transition is characterized by a progressive phase decoupling at the sample's weak links resulting effectively to decreasing total superconducting volume and, correspondingly, increasing normal regions where the flux lines can "leak" into. In region III, this competition is manifested by a decreasing magnetoresistance in the approach to T_c. This means that, in this region, the competition results to an effective decrease of vortex motion. In region IV, the sample is in the normal state where full penetration of the electric field is permitted and the applied current is dissipated according to the sample's normal state properties.

The isothermal I-V profiles obtained with varying applied fields are shown in Fig. 3. Four I-V measurements were obtained at temperatures chosen within region II for each magnetic application of 1.25 and 0.1 T. For an unpinned but damped flux-line lattice, the average velocity of the flux lines v_f is proportional

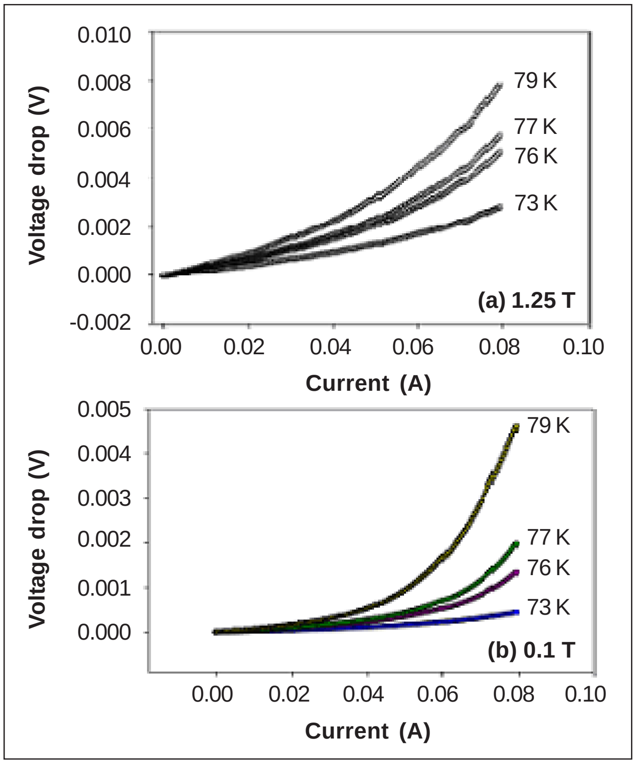

Fig. 3. The *I*-*V* plots at different temperature values with applied magnetic fields of (a) 1.25 and (b) 0.1 T show nonlinearity associated with flux motion.

to the current density $j = j_c$, and one obtains a linear relationship between *V* and *I*, noting that the electric field *E* due to vortex motion causes the measurable voltage drop *V*. When pinning is important, the average velocity associated with the thermally activated jumps of flux lines, so *E* is also exponentially dependent on the barrier *U*(*j*) as is *V* [7]. That is,

$$V = V_0 \exp\left(-Uk_B T\right) \qquad (2)$$

where

$$V_0 = \frac{V_0 l_{\text{hop}} B L_{\text{creep}}}{c} \qquad (3)$$

Here, l_{hop} is the vortex hopping distance, *B* is the applied magnetic field, L_{creep} is that length of the sample, which contributes to the flux creep and c is the speed of light.

Thus, flux creep is generally associated with a highly nonlinear *I*-*V* relationship, as the profiles in Fig. 3 show, dictated by the specific dependence of *U* on *I* and by the exponential dependence of *E* (or *V*) on *U*. As further depicted by the profiles, the voltage drop measured with the same magnitude of current increases with increasing temperature, consistent with the magnetoresistance data.

From Eq. (2), the current dependence of the potential barrier was obtained from the isothermal *I*-*V* data using

$$U\left(I\right) = -k_B T \ln\left[V\left(I\right)\right] + \alpha \qquad (4)$$

where a is current independent and equal to

$$\alpha = k_B T \ln\left(V_0\right) . \qquad (5)$$

Figures 4 shows, in (*U*–a) against *I* plot, the current dependence of the barrier *U* at different temperatures in the flux creep regime with (a) 1.25 and (b) 0.1 T applied magnetic fields. With temperature, *U*–a decreases for both applied magnetic fields. This behavior is consistent with the KA thermally activated mechanism. All profiles, however, depict nonlinearity of the barrier *U* on *I*. This dependence is different from the original Kim-Anderson flux creep model assumption of a linear *U*(*j*). But, as first recognized by

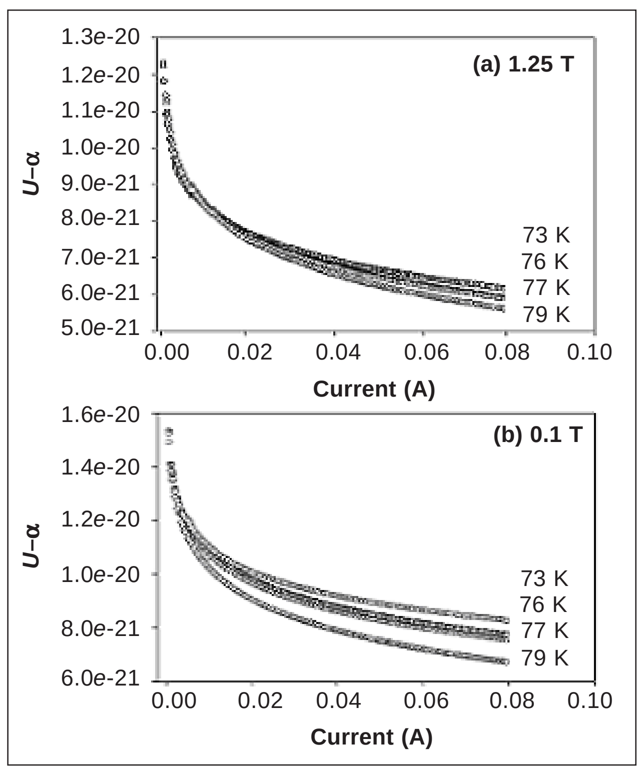

Fig. 4. The potential barrier *U* diverges as current *I* approaches zero for both applied fields.

Beasley et al. [8] and recently strongly put forward by Landau and Ott [9], the linearity of U with j is only a first approximation and a more realistic barrier should exhibit a nonlinear dependence on current. There is, further, no physical reason in the KA description for anticipating a linear $U(j)$.

The divergence of the flux creep potential barrier U as I approaches zero is explained by the collective creep theory in terms of a state of immobility of an infinitely large flux bundle. The vortex-glass model relates this immobility to a thermodynamic phase transition from an initially mobile state. A divergent U from Eq. (4), however, corresponds to a zero measured voltage drop, which may be expected of a moving vortex system producing zero net electric field due to random hopping. In the presence of an applied current, an effective nonzero electric field can only be expected because flux creep is facilitated towards the direction of the driving Lorentz force.

Furthermore, the electrodynamics of the collective creep theory predicts an inverse power-law dependence of the flux creep potential barrier U on j, with a temperature-dependent universal exponent. Figures 5(a) and 5(b) show, however, that the barriers obtained at 79 K with 1.25 T and 73 K with 0.1 T, respectively, fit perfectly to the logarithmic function

$$y = a + b\ln(x) \tag{6}$$

To further investigate the rate of change of the potential barrier with respect to current, plot of dU/dI versus current was determined. The collapse to a single curve of $d(U–a)/dI$, for both with 1.25 T in Fig. 6(a) and 0.1 T in Fig. 6(b), shows that at all temperatures, U varies with I in the same manner. Moreover, this collapse is consistent with the simple Anderson-Kim thermally activated mechanism with

$$U(j,t) = u(j)u(t) \tag{7}$$

where $u(j)$ is the function determining the dependence of U on applied current j and $u(T)$ determines U with temperature T.

It was noted earlier that in the temperature regime of the observed mixed state where the sample undergoes an intrinsic transition to the normal state—region III in Fig. 2—an increasing potential barrier with temperature could be anticipated where the magnetoresistance profiles obtained without prior use of the Anderson-Kim model, manifests a decreasing behavior with temperature. It was, however, pointed out that this barrier could not be the true flux creep barrier since an increasing barrier with temperature only relates to a decreasing superconducting volume or an increasing normal region. Figure 7 shows the apparent barrier at 82 and 85 K, obtained through the same procedure using the Anderson-Kim flux creep equation. Indeed, the barrier increases rather than decrease with temperature, consistent with the decreasing magnetoresistance.

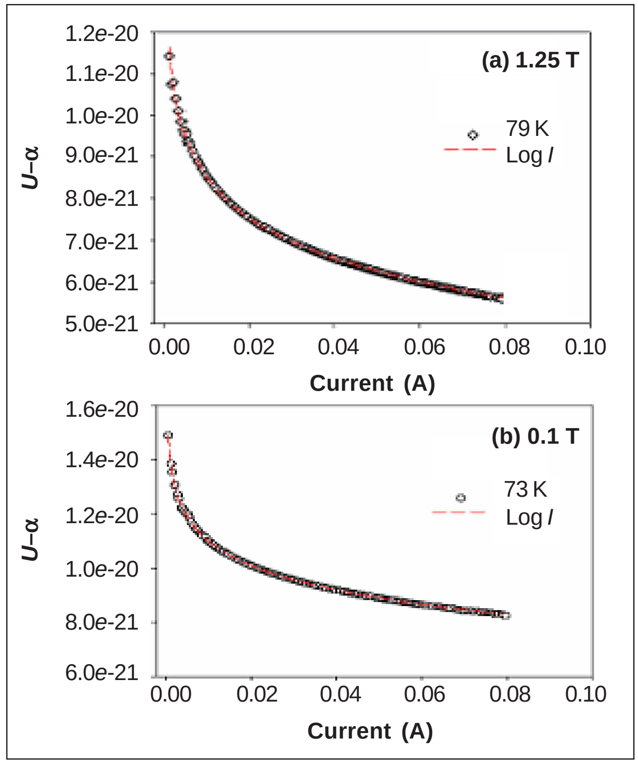

Fig. 5. The potential barrier U behaves logarithmically with current I at (a) 79 and (b) 73 K with 1.25 and 0.1 T applied fields, respectively.

CONCLUSIONS

The flux creep process in $Bi_2Sr_2C_aCu_2O_{8+d}$ can be described and analyzed using the Anderson-Kim approach. Magnetoresistance profiles exhibit peaked

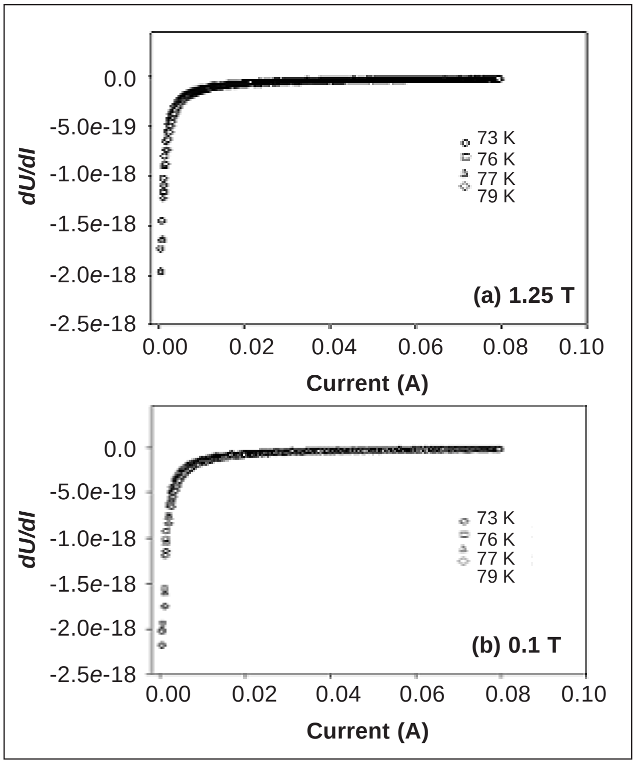

Fig. 6. The potential barrier *U* behaves in the same manner for all temperature values at (a) 79 and (b) 73 K with applied fields of 1.25 and 0.1 T, respectively.

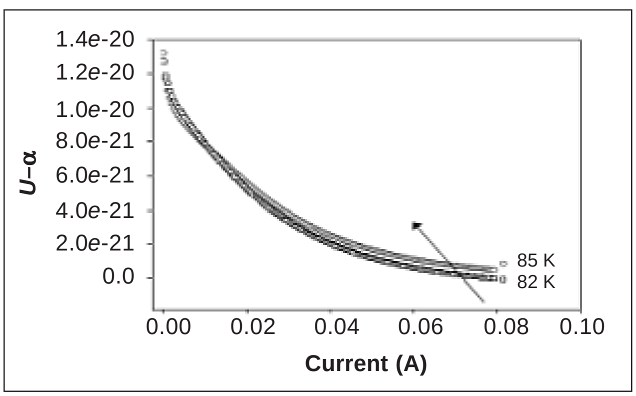

Fig. 7. The potential barrier *U* decreases with increasing temperature in the region of decreasing magnetoresistance.

behavior due to competing mechanisms of flux motion and sample-intrinsic transition to the normal state near T_c. In the temperature range where this competition occurs, the potential barrier increases with temperature since the increasing normal regions where vortices peak into, and simultaneously, the decreasing superconducting volume should correspond to an effective decrease in flux creep. Flux creep potential barrier varies with *I* at all temperatures consistent with the Kim-Anderson description.

REFERENCES

Ambanta, R.I., 2004. *C*-axis oriented B1-2212 superconducting thin film using liquid powder deposition and growth by partial melting (Undergraduate thesis), March 2004.

Landau, I.L. & H.R. Ott, 2001. *Phys. Rev. B*. **63**: 184516.

Landau, I.L. & H.R. Ott, 2002. *Phys. Rev. B*. **65**: 064511.

Poole, C.P., et al., 1995. Superconductivity. San Diego, Academic Press.

Yeshurun, Y., A.P. Malozemoff, & A. Shaulov, 1996. *Rev. Mod. Phys*. **68**: 912.